Reactive and Functional Polymers 139 (2019) 9–16

Contents lists available at ScienceDirect

Reactive and Functional Polymers

journal homepage: www.elsevier.com/locate/react

# Synthesis and characterization of novel bio-based benzoxazines from gallic acid with latent catalytic characteristics

Mustafa Arslan*

*Department of Chemistry, Faculty of Arts and Sciences, Kirklareli University, TR-39000 Kirklareli, Turkey*

ARTICLE INFO

*Keywords:*
Polybenzoxazines
Ring-opening polymerization
Curing temperature
Gallic acid
Bio-based benzoxazine

ABSTRACT

A novel bio-based main chain benzoxazine with two oxazine rings and one phenolic hydroxyl group in the same aromatic ring was synthesized and characterized. The method includes the synthesis of polymeric benzoxazine precursors from simple chemicals such as gallic acid, gallic amide, 4,7,10-trioxa-1,13-tridecanediamine and formaldehyde by using traditional main chain synthesis methodology. The precursors were successfully characterized by the spectral and thermal investigations using $^{1}$H NMR, FTIR, GPC, DSC and TGA. The results demonstrated that phenolic hydroxyl groups in the benzene ring which are adjacent to the two oxazine rings have a great effect to reduce ROP temperature of benzoxazines. The clear reduction in ROP temperature was demonstrated by tracking exotherm in DSC analysis with an onset value at 126 °C. Moreover, thermal stability of the final products were investigated by TGA and high char yields observed.

## 1. Introduction

Among commonly used thermosetting resin systems (such as phenolics, epoxies, bismaleimides, cyanate esters, vinyl esters, and polyimides), polybenzoxazines (PBZs) has recently attracted much interest. PBZs are a class of polyphenolic thermoset resins and can be obtained by ring-opening polymerization (ROP) of the benzoxazine monomers without using any catalyst. These thermosetting materials have attracted interest in various scientific and industrial areas due to their superior properties such as high char yield, low shrinkage and humidity uptake, non-catalytic synthesis, limited by-product formation during curing and high glass transition temperatures. Most of the exclusive properties of PBZs are due to chain structure; the Mannich base bridges -$CH_2$-N(*R*)-$CH_2$- and the intra- and inter molecular hydrogen bonds between amine and the phenolic -OH groups. Polybenzoxazines can basically be synthesized by ROP of 1,3-benzoxazine monomers by thermal curing in the range of 150–250 °C depending on the benzoxazine monomer structure without using a catalyst [1] (Scheme 1).

Great versatility of monomer molecular design allows to synthesize novel monomers with various properties and specific functionalities [2–5]. Moreover, bio-based benzoxazine materials have taken excessive attention from the academy and industry for the development of less toxic and renewable polymers. Various benzoxazine polymers have been prepared with the properties of classical benzoxazine thermosets from inexpensive phenolic and amine derivatives such as cardanol [6–8], vanillin [9,10], guaiacol [11,12], eugenol [13–15], resorcinol [16], stearylamine [11], furfurylamine [17], chavicol [18], arbutin [19] and phthalonitrile [20–24]. In order to keep the interest to use a bio-based monomer, gallic acid (3,4,5-trihydroxybenzoic acid) can be used as a naturally occurring phenol. Gallic acid is a water-soluble phenolic structure which is existing in grapes and in the leaves of many plants and it is a well-known natural antioxidant that is a secondary polyphenolic metabolite [25–28]. A significant source of gallic acid is also tea which contains 4.5 g/kg weight in tea leaves [29,30].

The polymerization of the benzoxazine monomers is a cationic ring-opening process which is thermally catalyzed at high temperatures generally over 220 °C [31]. These curing temperatures are very high for industrial applications and can be reduced via some catalyst systems [32–36]. Liu described a new thermal latent curing strategy that stabilizes reactive benzoxazine-amine monomer blends by reaction equilibrium. The system provides long storage time and also short gel time at low temperature [37]. Yagci and *co*-workers investigated the effect of amine HCl salts as a catalyst and it was demonstrated that these salts cause sharp reduction in ring-opening polymerization temperature. Recently, the influence of nucleophilicity of counterions of amines HX salts was investigated and significant reduction detected for the curing temperature with a trend as $I^-$, $Br^-$, $Cl^-$ [38]. A naphthoxazine based latent catalyst was also described to reduce the ROP temperature. Basically, the system uses naphthoxazines as a curing-promoters which has a phenolic hydroxyl group with adjacent electron-withdrawing

* Corresponding author.
*E-mail address:* marslan@klu.edu.tr.

https://doi.org/10.1016/j.reactfunctpolym.2019.03.011
Received 16 January 2019; Received in revised form 28 February 2019; Accepted 9 March 2019
Available online 12 March 2019
1381-5148/ 

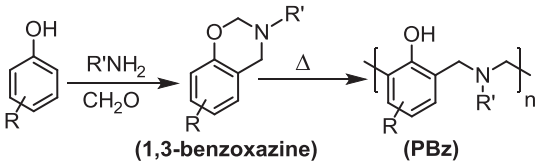


**Scheme 1.** Synthesis of 1,3-benzoxazines and corresponding PBZs by ring-opening polymerization.

groups and the high acidity of structure catalyze ROP of monomers [39,40]. The autocatalytic thermal polymerization behavior of benzoxazine monomers containing carboxylic acid functionalities was investigated by Ishida and Ronda [41–43]. Adding small amounts of carboxylic acid containing benzoxazine comonomers effectively catalyzes the thermal curing and decrease to the ring opening polymerization temperature.

The intra- and inter-molecular hydrogen bonds of oxazine rings provide unique and characteristic features to the benzoxazine monomers by reducing ROP temperatures [44]. Agag et al. developed a smart polybenzoxazine, known as *ortho*-amide functional benzoxazine. Interestingly, exceptional features of this class of benzoxazines was observed. The cationic ROP was performed at lower temperatures among traditional benzoxazines without adding initiator or catalyst. They assumed that the existence of intramolecular hydrogen bonding between an amide linkage and the adjacent oxazine unit acts as an internal incentive to trigger ROP. It behaves like a self-complementary initiator and reduce ROP temperature in a smart way. A o-trifluoroacetamide functional benzoxazine was synthesized to benefit its superior properties of *ortho*-functional benzoxazine to meta- and para-counterparts. ROP temperature was below 200 °C without mixing any catalyst and initiator and also benzoxazole formation occurred at extraordinarily low temperatures below 270 °C [45]. A series of ortho-, meta-, or para-methylol-functional benzoxazine isomers are synthesized and ROP properties investigated. The presence of methylol groups reduce ROP temperature. However, the highest reactivity is attributed to the *ortho*-functional monomer for the catalytic effect of the methylol group [46–48]. The effect of position (ortho-, meta-, or para-) of oxazine ring in the benzoxazine spine was investigated by Endo and they found that when the benzoxazine monomer substituted with another benzoxazine unit as an alternative of functional group, meta-positioning has promising properties relative to their para and ortho counterparts (meta (225 °C) < ortho (239 °C) < para (251 °C)). They proposed a different ROP mechanism for lowering curing temperature in meta position which involves an intramolecular electrophilic substitution of iminium ion, resulting in aza-cyclic rings along with phenolic Mannich bridges [49,50]. Hartwig and *co*-workers prepared a resorcinol-based polybenzoxazine by a cationic polymerization with thermo latent super acids and the curing temperature of the system was impressive [51]. More recently, Zhu et al. synthesized pyrogallol-based difunctional benzoxazines (PG-FA and PG-A) with a phenolic hydroxyl between two oxazine rings appending to the same benzene ring. The phenolic hydroxyl exhibited an important role on ROP. The intra- and inter-molecular hydrogen bonds of hydroxyls converted into hydroxyl-pi intramolecular interactions, which formed the free phenolic hydroxyls. The catalytic activity of the hydroxyls accelerates the opening of oxazine ring and the attack of the carbenium ions to active position of the pyrogallol forms polybenzoxazines [52].

In these functional benzoxazine structures, hydroxyl of the phenolics have a significant status as an autocatalytic group and decrease ROP temperature. As we mentioned above, phenolic nucleophiles have a significant effect on ROP and among them pyrogallol is one of the best structures [36,52]. In the light of this information, first time main-chain type benzoxazine with a phenolic hydroxyl group between two oxazine ring could be obtained and gallic acid is the best candidate being as a bio-based molecule. By this means, gallic acid, gallic amide, 4,7,10-trioxa-1,13-tridecanediamine and formaldehyde were used to synthesize bio-based main-chain benzoxazine and the polymerization behavior was investigated in detail.

## 2. Experimental

### 2.1. Materials

3,4,5-Trihydroxybenzoic acid (gallic acid) (Aldrich, 99%), 4,7,10-trioxa-1,13-tridecanediamine (Aldrich, ≥98%), paraformaldehyde (Acros, 96%), *p*-toluidine (Aldrich, 99.6%), sodium hydroxide (Aldrich, ≥97%), ethanol (Aldrich, ≥99.5%), toluene (Carlo Erba, 99.5%), chloroform (Acros, 99 + %), hexane (Aldrich, 95%), *p*-xylene (Aldrich, ≥99%), celite (Aldrich), 1,4-dioxane (Riedel-de Haen, 99.5%), diethyl ether (≥98%, Aldrich), deuterium oxide (Aldrich, $D_2O$, 99.9 atom% D), tetrahydrofuran (THF, VWR Chemicals, 99.7%), *N,N*-dimethylformamide (DMF, Merck), dichloromethane (DCM, VWR Chemicals, 99.9%).

### 2.2. Measurements

The $^1$H NMR spectra of the monomer and polymers were measured at room temperature in $CDCl_3$ or DMSO-$d_6$ with $Si(CH_3)_4$ using a 500 MHz NMR (Agilent NMR System VNMRS). Thermal gravity analysis was performed on Setaram Sensys Evo TG-DSC at a heating rate of 10 °C/min from 30 to 900 °C under nitrogen. Differential scanning calorimetry (DSC) measurements were taken using a PerkinElmer Diamond DSC and Setaram Sensys Evo TG-DSC under a scanning rate of 10 °C/min, covering temperatures of 30–320 °C. The Fourier transform infrared (FTIR) spectroscopy measurements were recorded as 4 scans using a PerkinElmer FTIR Spectrum One spectrometer. Gel permeation chromatography (GPC) measurements were performed on a TOSOH EcoSEC GPC system equipped with an auto sampler system, a temperature-controlled pump, a column oven, a refractive index (RI) detector, a purge and degasser unit and TSK gel superhZ2000, 4.6 mm ID × 15 cm × 2 cm column. Tetrahydrofuran was used as an eluent at flow rate of 1.0 mL min$^{-1}$ at 40 °C. Refractive index detector was calibrated with polystyrene standards having narrow molecular-weight distributions. Data were analyzed using Eco-SEC Analysis software.

### 2.3. Syntheses

#### 2.3.1. Synthesis of gallic acid-based main chain benzoxazine (GA-Bz)

The synthesis was performed according to the literature with a few modifications [52]. In a 100 mL round flask, paraformaldehyde (47 mmol, 1.412 g) and $H_2O$ (5.5 g) were added and the pH of the medium was adjusted to 8–9 with NaOH solution. The colloidal mixture was heated and stirred until to obtain a clear phase. 4,7,10-Trioxa-1,13-tridecanediamine (11,7 mmol, 2.590 g) was dissolved in 1,4-dioxane and added into the flask at room temperature and left to mix for 1 h. Then, 3,4,5-trihydroxybenzoic acid was (11.7 mmol, 2 g) put into the mixture and stirred at 70 °C for 80 h. The formed solid was removed by filtering. The solvent was completely evaporated using a rotary evaporator. The remaining product dissolved in a tiny $CHCl_3$ and precipitated by the dropwise addition into the excess diethyl ether (200 mL). The precipitation process was performed for two times. Precipitated polymers were collected by decantation and dried in vacuum at room temperature.

#### 2.3.2. Synthesis of gallic amide monomer (G-Amd)

Gallic acid-based amide synthesis was achieved according to the literature [53]. In a 50 mL round flask, 3,4,5-trihydroxybenzoic acid (5.88 mmol, 1 g) and *p*-toluidine (5.88 mmol, 0.629 g) dissolved in 20 mL *p*-xylene. The mixture was refluxed for 24 h. Xylene was removed using a rotary evaporator. The product was dissolved in $CH_2Cl_2$ and filtrated through a pad of celite. Solvent evaporated and the product was dried in vacuum at room temperature.

*2.3.3. Synthesis of gallic amide-based main chain benzoxazine (G-Amd-Bz)*

In a 100 mL round flask, G-Amd (1.93 mmol, 0.5 g) monomer, paraformaldehyde (7.72 mmol, 0,232 g) and 4,7,10-trioxa-1,13-tridecanediamine (1.93 mmol, 0.425 g) were added and dissolved in 50 mL 1,4-dioxane. The flask was refluxed for 4 h. The formed solid was removed by filtering. The solvent was evaporated using a rotary evaporator. The product was concentrated and precipitated by the dropwise addition into the 100 mL excess diethyl ether. The solid was collected after decantation and dried at room temperature under vacuum overnight.

## 3. Results and discussion

Among high performance polybenzoxazine thermosets, *o*-amide functional benzoxazines known as a smart class of such materials. The precursors could be synthesized by various combinations of phenolics and amine derivatives to form monomers, oligomers, main-, side- and end-chain-type polymers [54,55]. ROP of benzoxazines commence by the cleavage of methylene bridge on the oxazine ring to form a cationic intermediate by thermal activation. These cationic species can then attack N-, O- and aryl groups to yield polybenzoxazines. Commonly, high curing temperatures are required to start ROP. Interestingly, *o*-amide functional benzoxazines show ROP at lower temperatures without adding any initiators and/or catalyst. Intramolecular hydrogen bonding between amide functionality and neighboring oxazine ring make the structure a self-complementary initiator by acting as an internal stimulus [55]. Therefore, a novel bio-based amide-functional main chain benzoxazine polymer precursors were synthesized with the appropriate structures.

The first strategy was established by the synthesis of gallic acid-based benzoxazine with the reaction of 3,4,5-trihydroxybenzoic acid, 4,7,10-trioxa-1,13-tridecanediamine and paraformaldehyde (Scheme 2).

### 3.1. Preparation of GA-Bz and structural characterization

The chemical structure of the polymer was confirmed by spectral and thermal analysis. As it can be seen from the $^1$H NMR shifts (Fig. 1), the signals emerged at 4.74 (O-$CH_2$-N) and 4.27 (Ar-$CH_2$-N) ppm are attributed to oxazine ring of GA-Bz. The chemical shifts of gallic acid aromatic protons located at 6.91 ppm was completely disappeared after reaction which supports to the formation of di-oxazine ring. The resonance signals of the 4,7,10-trioxa-1,13-tridecanediamine methylene protons also observed at 1.66 (C-$CH_2$-C), 2.55 (N-$CH_2$-C) and 3.43 (O-$CH_2$-C) ppm, respectively. DMSO-$d_6$ would form strong interaction with the phenolic hydroxyl and acid proton of GA-Bz. While the NMR shifts may be visible, it is not integrable [40]. Phenolic and carboxyl acid hydroxyl resonances are not detected or very slight because of inter- and intra-molecular hydrogen bonding.

As shown in Fig. 2, the characteristic bands of the benzoxazines emerged at 1325 $cm^{-1}$ ($CH_2$ wagging), 1102 $cm^{-1}$ (asymmetric stretching vibration of Ar-O-C) and 936 $cm^{-1}$ (out of plane distortion of oxazine unit). The band at 962 $cm^{-1}$ is allocated to the C − H out-of-plane bending of the benzene to which the oxazine ring is adjacent. The symmetric stretching vibrations of oxazine group (Ar-O-C) overlapped with Ar-OH and C-O-C vibrations at 1102 $cm^{-1}$. The broad vibration band between 2000 and 3710 $cm^{-1}$ is corresponds to the intra- and intermolecular hydrogen bonds of carboxyls and phenolics with O and N atoms. After synthesis, the formation of new bands clearly confirms the success of the reaction.

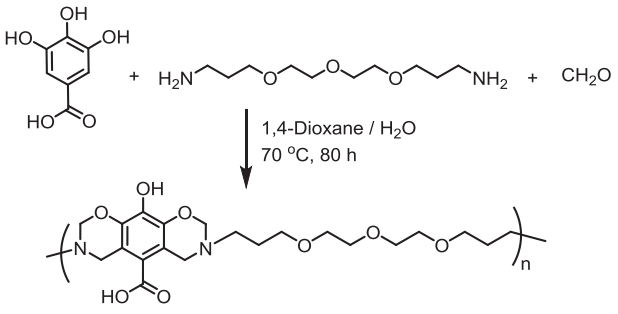


**Scheme 2.** Synthesis of gallic acid-based main chain benzoxazine (GA-Bz).

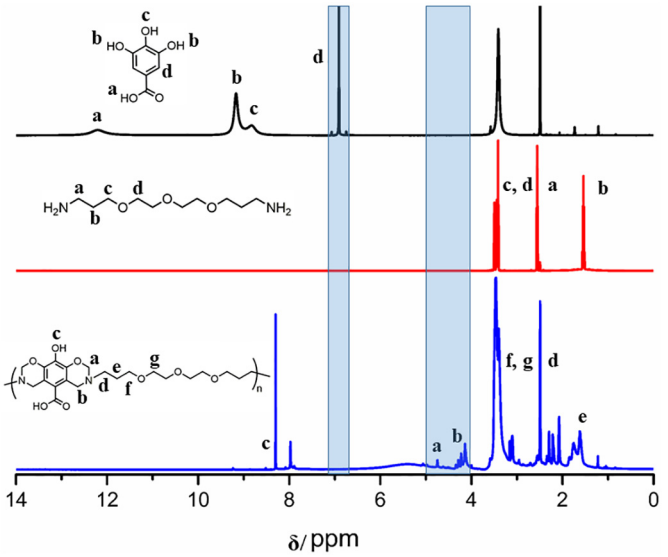


**Fig. 1.** $^1$H NMR spectra of 3,4,5-trihydroxybenzoic acid, 4,7,10-trioxa-1,13-tridecanediamine and GA-Bz.

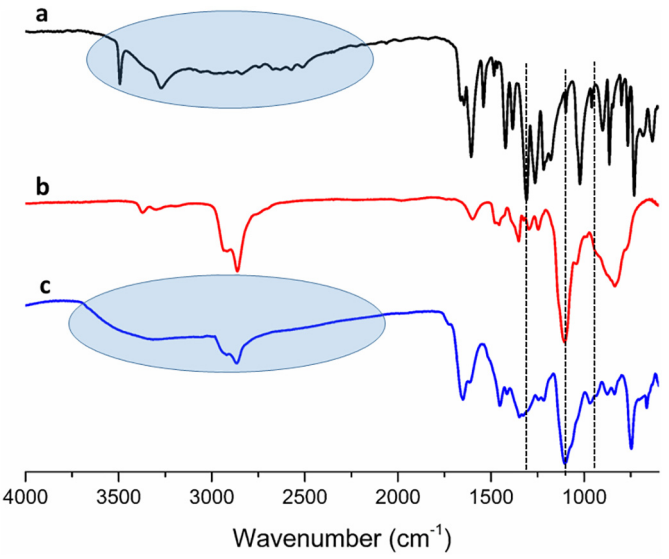


**Fig. 2.** FT-IR spectra of 3,4,5-trihydroxybenzoic acid (a), 4,7,10-trioxa-1,13-tridecanediamine (b) and GA-Bz (c).

The ROP temperature of benzoxazines are mostly lay between 160 and 260 °C which is depending to the functionalities present on the structure. The functional groups such as carboxylic acid, alcohol and phenolic hydroxyl would decrease the ROP temperature by showing a lower exothermic peak in DSC [56–58]. Phenolic hydroxyl groups have a significant role as a catalyst due to the activation effect. Moreover, *orto*-amide functional benzoxazines polymerize at much lower temperatures without added initiators and/or catalyst [45,55,59]. Therefore, the hydrogen bonding system which contains a five-membered-ring with the amide linkage and the attached oxazine ring would be act a “reinforced incentive” to encourage the ring opening polymerization. In our system, GA-Bz is probably forming an intra- and intermolecular

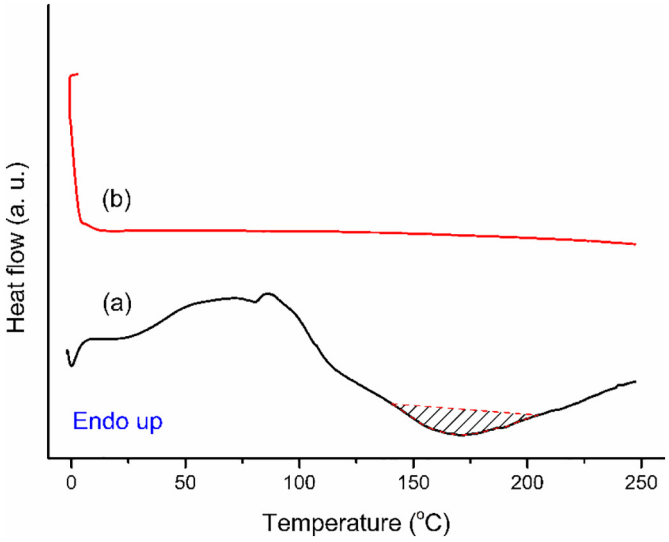


**Fig. 3.** DSC thermographs of GA-Bz (a) and cured GA-Bz (b).

hydrogen-bonding system involving the phenolic hydroxyl at each site of the gallic acid monomer. As you see from the Fig. 3, this fact is demonstrated by observing lower ROP temperature of the GA-Bz. GA-Bz has an exotherm with a maximum of 169 °C, which is related to contribution of the phenolic and acid groups. The similar catalytic effect was also observed on the on-set and end-set temperatures.

Main-chain polymer formation was monitored by using a gel permeation chromatography (GPC). The number average molecular weight of GA-Bz was measured as 4950 Da ($M_w/M_n$: 1.30) (Table 1). According to the GPC results each GA-Bz chains were modified by 11 gallic acid and diamine monomer after reaction. This data corresponds to the soluble part of the polymer precursor in THF. The monomodal narrow molecular weight distribution and the clear shift were observed as a result of the characteristics of step-growth polymerization and also it can be inferred that no significant side reactions accorded.

Main-chain benzoxazines could be easily synthesized through using a diphenol and diamine-based structures by means of the one-step condensation of reaction components such as phenols, amines and formaldehyde. On the other hand, direct reaction of amine and formaldehyde causes to the formation of insoluble triazine network. Concurrently, carboxyl groups can react with the primary amines to produce an amide structure. Two hydroxyl and one carboxyl functionality of the gallic acid monomer force to behave a crosslinker. It effects the reaction yield. Therefore, another strategy was applied to synthesis main-chain benzoxazine. Among many methods, the simplest way is that amides can be synthesized by the reaction of amines with acid chlorides and carboxyl acids. Thus, gallic acid monomer was reacted with *p*-toluidine to obtain an amide functional monomer and subsequently, it was reacted with 4,7,10-trioxa-1,13-tridecanediamine and paraformaldehyde to form benzoxazine polymer. Hence, we could synthesize benzoxazine with high yields by eliminating side reactions of carboxyl groups during the classical benzoxazine condensation reactions.

**Table 1**
Molecular weight characteristics of the polymers.

| Run | Polymer | $M_{n\ (GPC)}$[a] | PDI[a] |
|---|---|---|---|
| 1 | GA-Bz | 4950 | 1.30 |
| 2 | GA-Amd-Bz | 4420 | 1.23 |

[a] Determined by GPC, according to polystyrene standards.

### 3.2. Preparation of G-Amd-Bz and structural characterization

The chemical structure of G-Amd monomer (Scheme 3) was confirmed by spectral analysis. As can be seen from the NMR spectra (Fig. 4) characteristic carboxyl acid proton shifts at 12.18 ppm disappeared after reaction. The amide proton around 9.10 ppm overlapped with the hydroxyl protons of gallic acid with an increment of the peak intense. Moreover, new resonance signals attributed to the *p*-toluidine methyl and aromatic protons were located at 2.07 and 6.41–6.71 ppm, respectively.

As shown in Fig. 5, the characteristic amide carbonyl and amide II band emerged at 1725 and 1500 $cm^{-1}$, respectively [60]. The OH stretch of COOH dimer hydrogen band causes a very broad absorption. The antisymmetric coupled OH stretching at 3270 $cm^{-1}$ and C=O stretch overtone at 3484 $cm^{-1}$ were disappeared after amide formation. In addition, the characteristic overtone pattern of the COOH group around 2600 $cm^{-1}$, bend/stretch at 1485 $cm^{-1}$, stretch/bend at 1250 $cm^{-1}$ and out-of-plane wag in acid dimer at 910 $cm^{-1}$ were disappeared after amide formation. However, N–H stretching vibrations of the primary amine was not observed at 3360 $cm^{-1}$. Consequently, both NMR and IR results indicate the formation of G-Amd.

$^1$H NMR, FTIR, DSC and GPC analysis were performed to identify the chemical structure of G-Amd-Bz (Scheme 4). The protons resonating at 4.78 (b) (O-$CH_2$-N) and 4.18 (c) ppm (Ar-$CH_2$-N) is a clear evidence for the formation of oxazine ring. Furthermore, the hydroxyl peaks of G-Amd monomers around 9.12 ppm are disappeared because of oxazine ring formation. Amide proton resonance signals shift to 8.30 ppm. Aromatic protons and methyl protons are also visible in the NMR spectra (Fig. 6). However, the resulting product contains small amount of impurities, despite efforts to eliminate the starting materials.

As shown in overlaid FT-IR spectra (Fig. 7), the characteristic bands of the benzoxazines emerged at 1410 ($CH_2$ wagging), 1104 (asymmetric stretching of Ar-O-C) and 946 $cm^{-1}$ (out of plane vibration of oxazine unit). The symmetric stretching vibrations of oxazine group (Ar-O-C) overlapped with Ar-OH and C-O-C vibrations at 1104 $cm^{-1}$. The obvious decrement was observed between 2000 and 3710 $cm^{-1}$ which is belong to phenolic hydroxyls. The characteristic carbonyl and amide band were also visible at 1725 and 1500 $cm^{-1}$, respectively. The intensity of the amide carbonyl band was reduced as a result of polymeric structure.

The number average molecular weight of G-Amd-Bz polymer was measured as 4420 Da ($M_w/M_n$: 1.23) via GPC analysis (Table 1). Each G-Amd-Bz chains were modified by nearly 9 gallic amid and diamine monomer according to the GPC thermogram. The monomodal narrow molecular weight distribution and the clear shift were observed as a result of the characteristics of step-growth polymerization.

### 3.3. Curing behavior of GA-Bz and G-Amd-Bz

Depending on the functional groups, the ring-opening polymerization temperatures of the benzoxazines range between 160 and 260 °C and can be monitored as an exotherm. Therefore, ring-opening polymerization temperatures of GA-Bz and G-Amd-Bz were investigated using DSC under $N_2$ atmosphere (Fig. 8). G-Amd-Bz displayed an exotherm peak with an onset at 126 °C and an end-set at 167 °C. The curing maximum was also detected as 151 °C. The overall curing exotherm quantity is 55 J/g. Following curing of G-Amd-Bz, the second run did not display any curing exotherm. It demonstrates the depletion of the oxazine units in the first process during thermal treatment.

The polymerization kinetics of GA-Bz and G-Amd-Bz have been examined and followed with a heat evaluation in DSC at different heating rates of 2, 5, 10, 15 and 20 °C/min as shown in Fig. 9. As given in Table 2, the maximum curing temperature peak $T_{max}$ at all the heating rates follows the sequence of 129, 140, 151, 155, 160 °C, respectively. These exotherms were lower than classic benzoxazine monomers and the characteristics are mainly due to the gallic unit,

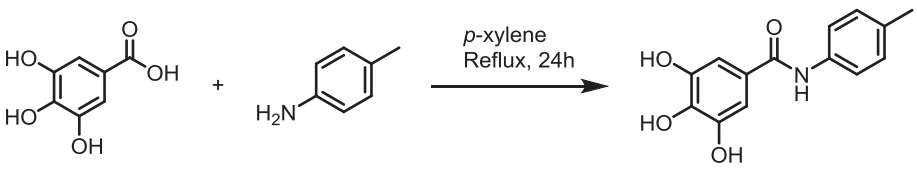


**Scheme 3.** Synthesis of gallic amide monomer (G-Amd).

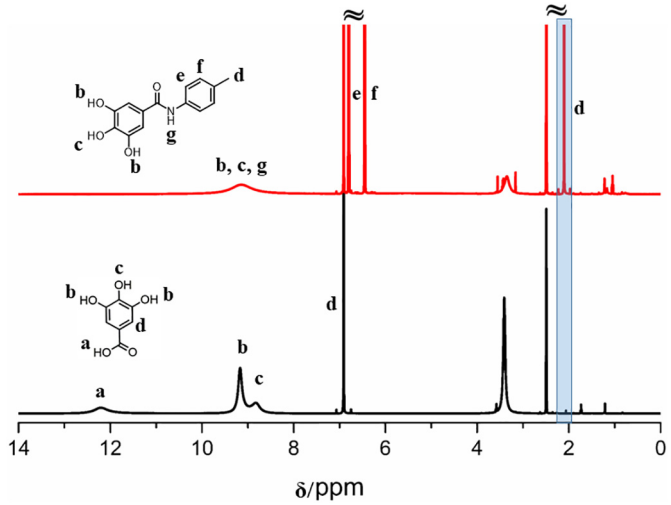


**Fig. 4.** $^{1}$H NMR spectra of gallic acid and G-Amd.

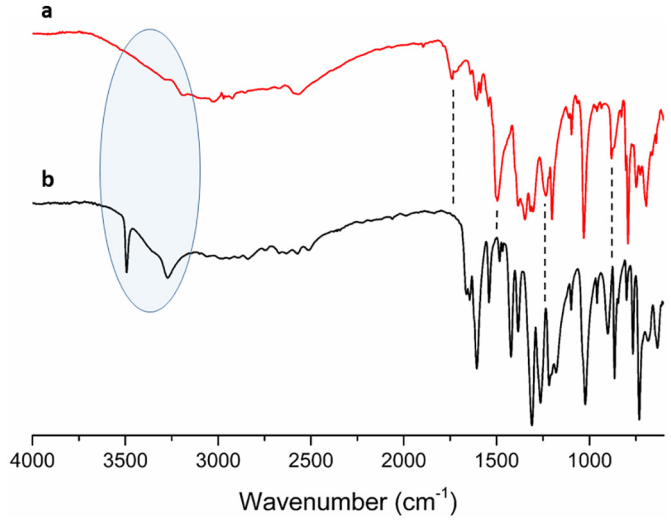


**Fig. 5.** FT-IR spectra of 3,4,5-trihydroxybenzoic acid (b) and G-Amd (a).

which has a free phenolic hydroxyl and carbonyl group and the differences in the reactivity. Moreover, DSC heat flow is proportional to the reaction rate according to the non-isothermal DSC kinetic analysis. The activation energy for the polymerization was studied using the well-known Kissinger and Ozawa methods by different research groups [58,61–63]. The naphtoxazine, amide and imide functional benzoxazines has showed lower activation energy and curing temperature [40,59]. The thermograms represent that the exothermic ROP peaks shift to a lower temperature with the decrease of heating rate as expected. The low ROP temperatures suggest that G-Amd-Bz is easy to be activated to polymerize and it is compatible with the literature [40,52,59].

### 3.4. Thermal properties of GA-Bz and G-Amd-Bz

Thermal stability of the GA-Bz and G-Amd-Bz polymers was explored using thermo-gravimetric analysis (TGA) under $N_2$ atmosphere. The TGA traces of the polymers are shown in Fig. 10 and related results are collected in Table 3. The cured modified GA-Bz and G-Amd-Bz polymers obviously showed higher char yields. Pristine 4,7,10-trioxa-1,13-tridecanediamine has 0% char yield at 900 °C and has nearly vaporized at 900 °C. GA-Bz and G-Amd-Bz displayed char yields as 36.5% and 39%, respectively. G-Amd-Bz exhibits rather higher char yield most possibly due to the large amount of benzoxazine component per polymer chain. TGA results clearly disclose that integration of benzoxazines into polymer considerably improved the char yield. The expected product structure is a phenoxy type polybenzoxazine. Basically, Friedel–Crafts reaction takes place through the reaction of oxygen, nitrogen and the unoccupied benzene ortho or para position to produce a phenoxy or phenolic structure. In this study, benzoxazine aromatic ring is all-substituted. For this reason, polymerization can proceed through the oxygen atom to produce a phenoxy type polybenzoxazine structure.

## 4. Conclusion

A novel gallic acid-based main chain bio benzoxazines with two oxazine rings and one phenolic hydroxyl group in the same benzene ring was synthesized with different methods. The synthesized main-chain polymers indicate thermally stimulated curing at much lower than that of conventional benzoxazines. The results demonstrated that it is possible to reduce the ROP temperature of main chain benzoxazine polymers if the design is accomplished carefully. In the strategy, gallic acid based benzoxazine were synthesized through classic main chain benzoxazine precursor synthesis approach using gallic acid, gallic amide, diamine and formaldehyde. The reaction yield of gallic acid-based monomer was found low to produce a main chain polymer; thus, this compound converted to amide derivative and then used for the benzoxazine synthesis. Fortunately, the results indicated that free phenolic hydroxyls have excellent catalytic effect on the ring opening polymerization temperatures. The latent catalyst quality of hydroxyls was studied by tracking exotherm peak in DSC thermogram. Thermal analysis revealed the reduced maximum ROP temperatures 129, 140, 151, 155 and 160 °C at different heating rates of 2, 5, 10, 15 and 20 °C/min, respectively. Hydrogen bond interactions (intra- and inter-) of the free phenolic hydroxyl displayed a significant role on the ring-opening polymerization temperature. Apart from catalytic benefits, cured GA-Bz and G-Amd-Bz revealed high char yield as much as 39% at 900 °C. Consequently, free phenolic hydroxyl bearing benzoxazines have notable potential to reduce ROP temperature of benzoxazines acting as latent catalyst type, and the process is effective and cheap to extend industrial applications of high performance thermosets.

## Data availability

The raw/processed data required to reproduce these findings cannot be shared at this time as the data also forms part of an ongoing study.

## Acknowledgment

The author would like to thank Kirklareli University, Research Fund, for financial support (KLUBAP-129).

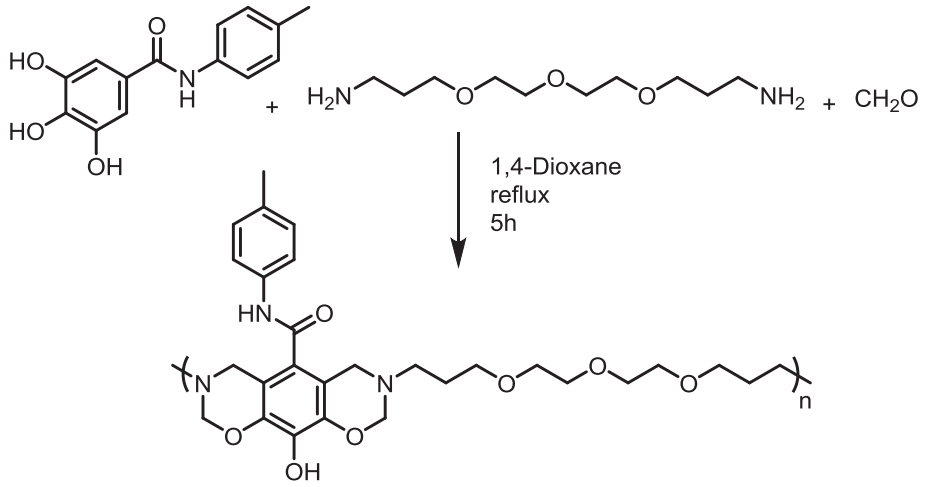


**Scheme 4.** Synthesis of gallic amide-based main chain benzoxazine (G-Amd-Bz).

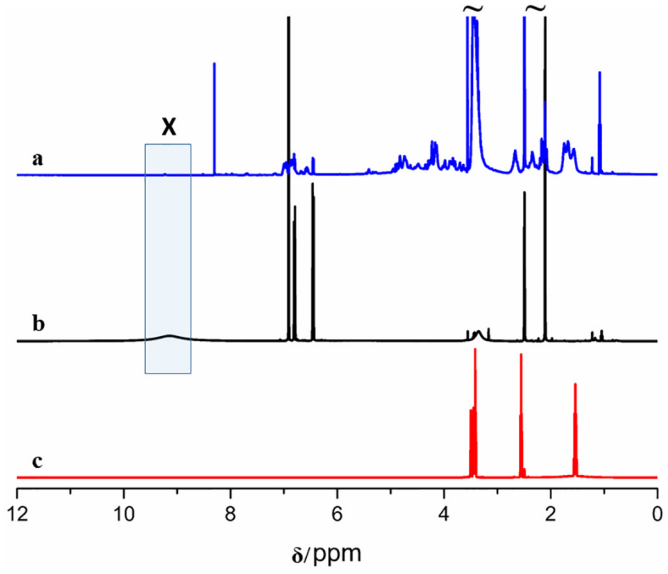


**Fig. 6.** $^1$H NMR spectra of 4,7,10-trioxa-1,13-tridecanediamine (c), G-Amd (b) and G-Amd-Bz (a).

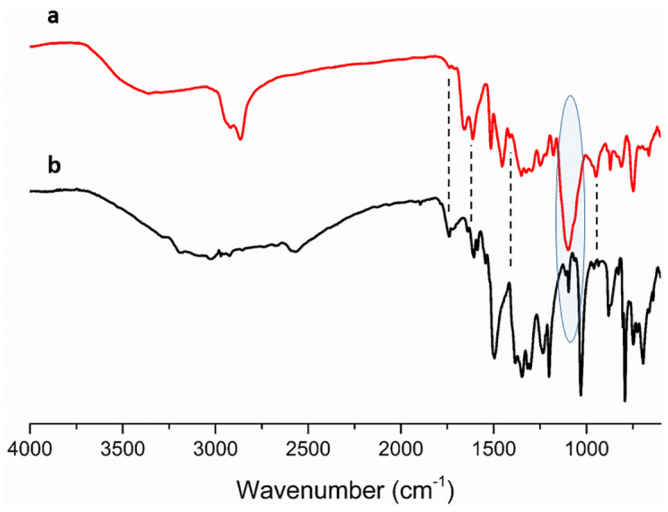


**Fig. 7.** FT-IR spectra of G-Amd (b) and G-Amd-Bz (a).

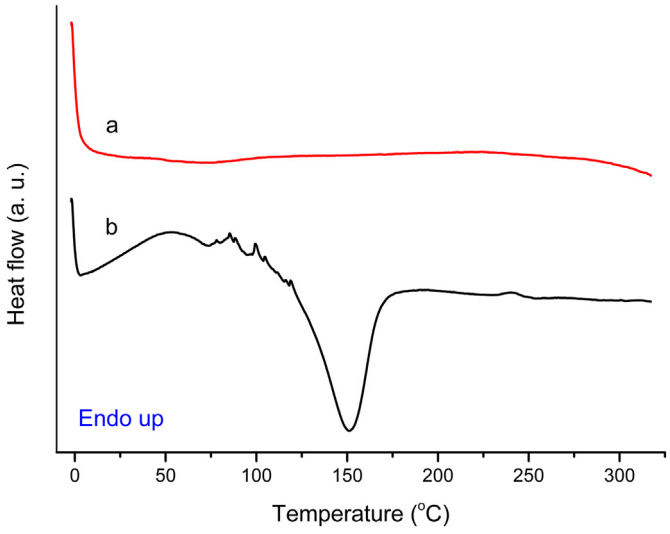


**Fig. 8.** DSC thermographs of G-Amd-Bz (b) and cured G-Amd-Bz (a).

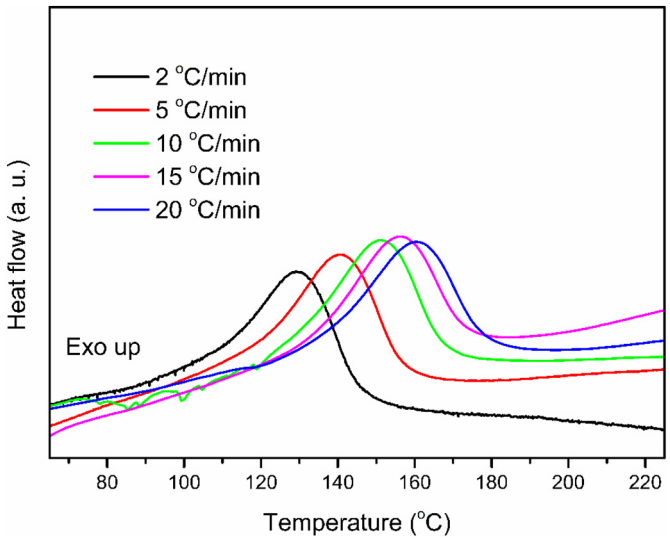


**Fig. 9.** DSC thermographs of G-Amd-Bz at various heating rates.

**Table 2**
DSC[a] characteristics of G-Amd-Bz and GA-Bz.

| Entry | Heating rate (°C/min) | On-set of curing (°C) | End-set of curing (°C) | Maximum curing (°C) | $\Delta H$ (J/g) |
|---|---|---|---|---|---|
| G-Amd-Bz | 2 | 98 | 143 | 129 | −68 |
| | 5 | 119 | 156 | 140 | −62 |
| | 10 | 126 | 167 | 151 | −55 |
| | 15 | 132 | 173 | 155 | −47 |
| | 20 | 134 | 178 | 160 | −53 |
| GA-Bz | 2 | 142 | 149 | 145 | −9 |
| | 5 | 130 | 210 | 150 | −53 |
| | 10 | 152 | 198 | 170 | −20 |
| | 15 | 122 | 216 | 171 | −18 |
| | 20 | 131 | 213 | 174 | −12 |

[a] DSC thermograms were collected under 20 mL·min$^{-1}$ $N_2$ flow and various (2, 5, 10, 15, 20) °C·min$^{-1}$ heating rate.

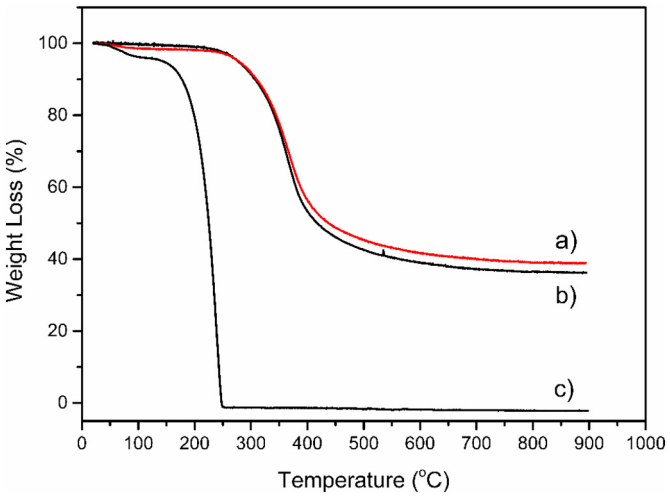


**Fig. 10.** TGA curves of cured G-Amd-Bz (a), GA-Bz (b) and trioxa-1,13-tridecanediamine (c).

**Table 3**
Thermal characteristics of cured GA-Bz and G-Amd-Bz polymers determined by TGA.

| Polymer | $T_{5\%}$ (°C) | $T_{10\%}$ (°C) | $T_{max}$ (°C) | $Y_c$ (%) |
|---|---|---|---|---|
| GA-Bz | 277 | 306 | 360 | 36.5 |
| G-Amd-Bz | 278 | 310 | 365 | 39 |

$T_{5\%}$: The temperature for which the weight loss is 5%, $T_{10\%}$: The temperature for which the weight loss is 10%, $T_{max}$: The temperature for which the weight loss is maximum, $Y_c$: Char yields at 900 °C under nitrogen atmosphere.

## References


[1] N.N. Ghosh, B. Kiskan, Y. Yagci, Polybenzoxazines—New high performance thermosetting resins: synthesis and properties, Prog. Polym. Sci. 32 (11) (2007) 1344–1391.
[2] M. Arslan, A. Motallebzadeh, B. Kiskan, A.L. Demirel, I.V. Kumbaraci, Y. Yagci, Combining benzoxazine and ketene chemistries for self-healing of high performance thermoset surfaces, Polym. Chem. 9 (15) (2018) 2031–2039.
[3] M. Arslan, B. Kiskan, Y. Yagci, Recycling and self-healing of polybenzoxazines with dynamic sulfide linkages, Sci. Rep. 7 (1) (2017) 5207.
[4] B. Kiskan, Adapting benzoxazine chemistry for unconventional applications, React. Funct. Polym 129 (2018) 76–88.
[5] Y. Yagci, B. Kiskan, N.N. Ghosh, Recent advancement on polybenzoxazine—A newly developed high performance thermoset, J. Polym. Sci. A Polym. Chem. 47 (21) (2009) 5565–5576.
[6] E. Calò, A. Maffezzoli, G. Mele, F. Martina, S.E. Mazzetto, A. Tarzia, C. Stifani, Synthesis of a novel cardanol-based benzoxazine monomer and environmentally sustainable production of polymers and bio-composites, Green Chem. 9 (7) (2007) 754–759.
[7] S. Shukla, A. Mahata, B. Pathak, B. Lochab, Cardanol benzoxazines – interplay of oxazine functionality (mono to tetra) and properties, RSC Adv. 5 (95) (2015) 78071–78080.
[8] B.S. Rao, A. Palanisamy, Monofunctional benzoxazine from cardanol for bio-composite applications, React. Funct. Polym. 71 (2) (2011) 148–154.
[9] A. Van, K. Chiou, H. Ishida, Use of renewable resource vanillin for the preparation of benzoxazine resin and reactive monomeric surfactant containing oxazine ring, Polymer 55 (6) (2014) 1443–1451.
[10] N.K. Sini, J. Bijwe, I.K. Varma, Renewable benzoxazine monomer from vanillin: synthesis, characterization, and studies on curing behavior, J. Polym. Sci. Part A-Polym. Chem 52 (1) (2014) 7–11.
[11] C.F. Wang, J.Q. Sun, X.D. Liu, A. Sudo, T. Endo, Synthesis and copolymerization of fully bio-based benzoxazines from guaiacol, furfurylamine and stearylamine, Green Chem. 14 (10) (2012) 2799–2806.
[12] Y. Lou, Z. Zhao, Z. Chen, Z. Dai, F. Fu, Y. Zhang, L. Zhang, X. Liu, Processability improvement of a 4-vinlyguiacol derived benzoxazine using reactive diluents, Polymer 160 (2019) 316–324.
[13] P. Thirukumaran, A. Shakila, S. Muthusamy, Synthesis and characterization of novel bio-based benzoxazines from eugenol, RSC Adv. 4 (16) (2014) 7959–7966.
[14] L. Dumas, L. Bonnaud, M. Olivier, M. Poorteman, P. Dubois, Eugenol-based benzoxazine: from straight synthesis to taming of the network properties, J. Mater. Chem. A 3 (11) (2015) 6012–6018.
[15] L. Dumas, L. Bonnaud, M. Olivier, M. Poorteman, P. Dubois, Bio-based high performance thermosets: stabilization and reinforcement of eugenol-based benzoxazine networks with BMI and CNT, Eur. Polym. J. 67 (2015) 494–502.
[16] L. Dumas, L. Bonnaud, M. Olivier, M. Poorteman, P. Dubois, High performance bio-based benzoxazine networks from resorcinol and hydroquinone, Eur. Polym. J. 75 (2016) 486–494.
[17] Y.L. Liu, C.I. Chou, High performance benzoxazine monomers and polymers containing furan groups, J. Polym. Sci. Part A-Polym. Chem 43 (21) (2005) 5267–5282.
[18] L. Dumas, L. Bonnaud, M. Olivier, M. Poorteman, P. Dubois, Chavicol benzoxazine: ultrahigh Tg biobased thermoset with tunable extended network, Eur. Polym. J. 81 (2016) 337–346.
[19] L. Dumas, L. Bonnaud, M. Olivier, M. Poorteman, P. Dubois, Arbutin-based benzoxazine: en route to an intrinsic water soluble biobased resin, Green Chem. 18 (18) (2016) 4954–4960.
[20] A.Q. Dayo, A.R. Wang, M. Derradji, S. Kiran, A. Zegaoui, J. Wang, W.B. Liu, Copolymerization of mono and difunctional benzoxazine monomers with bio-based phthalonitrile monomer: curing behaviour, thermal, and mechanical properties, React. Funct. Polym 131 (2018) 156–163.
[21] A.Q. Dayo, X.M. Cao, W.A. Cai, S. Song, J. Wang, A. Zegaoui, M. Derradji, Y.L. Xu, A.R. Wang, W.B. Liu, L.D. Gong, Synthesis of benzophenone-center bisphenol-a containing phthalonitrile monomer (BBaph) and its copolymerization with P-a benzoxazine, React. Funct. Polym 129 (2018) 46–52.
[22] Y.L. Xu, A.Q. Dayo, M. Derradji, J. Wang, W.B. Liu, S. Song, T. Tang, Copolymerization of bisphthalonitrile/benzoxazine blends: curing behavior, thermomechanical and thermal properties, React. Funct. Polym 123 (2018) 97–105.
[23] J. Wang, T.T. Ren, Y.D. Wang, X.Y. He, W.B. Liu, X.D. Shen, Synthesis, curing behavior and thermal properties of fluorene-containing benzoxazines based on linear and branched butylamines, React. Funct. Polym 74 (2014) 22–30.
[24] H. Wang, J. Wang, X.Y. He, T.T. Ren, W.B. Liu, X.D. Shen, J.W. Bai, Synthesis and thermal properties of difunctional chiral and achiral benzoxazines, Acta Polym. Sin. (4) (2013) 450–455.
[25] K.C. Marquardt, R.R. Watson, Chapter 2 – polyphenols and public health, in: R.R. Watson, V.R. Preedy, S. Zibadi (Eds.), Polyphenols in Human Health and Disease, Academic Press, San Diego, 2014, pp. 9–15.
[26] O.I. Parisi, F. Puoci, D. Restuccia, G. Farina, F. Iemma, N. Picci, Chapter 4 – polyphenols and their formulations: different strategies to overcome the drawbacks associated with their poor stability and bioavailability, in: R.R. Watson, V.R. Preedy, S. Zibadi (Eds.), Polyphenols in Human Health and Disease, Academic Press, San Diego, 2014, pp. 29–45.
[27] E. Xia, X. He, H. Li, S. Wu, S. Li, G. Deng, Chapter 5 – biological activities of polyphenols from grapes, in: R.R. Watson, V.R. Preedy, S. Zibadi (Eds.), Polyphenols in Human Health and Disease, Academic Press, San Diego, 2014, pp. 47–58.
[28] V.R. Punithavathi, P.S.M. Prince, R. Kumar, J. Selvakumari, Antihyperglycaemic, antilipid peroxidative and antioxidant effects of gallic acid on streptozotocin induced diabetic Wistar rats, Eur. J. Pharmacol. 650 (1) (2011) 465–471.
[29] M.K. Unnikrishnan, V. Veerapur, Y. Nayak, P.P. Mudgal, G. Mathew, Chapter 13 – antidiabetic, antihyperlipidemic and antioxidant effects of the flavonoids, in: R.R. Watson, V.R. Preedy, S. Zibadi (Eds.), Polyphenols in Human Health and Disease, Academic Press, San Diego, 2014, pp. 143–161.
[30] H.-L. Huang, C.-C. Lin, K.-C.G. Jeng, P.-W. Yao, L.-T. Chuang, S.-L. Kuo, C.-W. Hou, Fresh green tea and gallic acid ameliorate oxidative stress in kainic acid-induced status epilepticus, J. Agric. Food Chem. 60 (9) (2012) 2328–2336.
[31] Y.X. Wang, H. Ishida, Cationic ring-opening polymerization of benzoxazines, Polymer 40 (16) (1999) 4563–4570.
[32] C. Liu, D. Shen, R.M. Sebastián, J. Marquet, R. Schönfeld, Catalyst effects on the ring-opening polymerization of 1,3-benzoxazine and on the polymer structure, Polymer 54 (12) (2013) 2873–2878.
[33] A. Sudo, S. Hirayama, T. Endo, Highly efficient catalysts-acetylacetonato complexes of transition metals in the 4th period for ring-opening polymerization of 1,3-benzoxazine, J. Polym. Sci. A Polym. Chem. 48 (2) (2010) 479–484.
[34] M. Arslan, B. Kiskan, Y. Yagci, Ring-opening polymerization of 1,3-benzoxazines via borane catalyst, Polymers 10 (3) (2018) 239.
[35] A. Kocaarslan, B. Kiskan, Y. Yagci, Ammonium salt catalyzed ring-opening polymerization of 1,3-benzoxazines, Polymer 122 (2017) 340–346.
[36] S. Nalakathu Kolanadiyil, M. Azechi, T. Endo, Synthesis of novel tri-benzoxazine

and effect of phenolic nucleophiles on its ring-opening polymerization, J. Polym. Sci. A Polym. Chem. 54 (17) (2016) 2811–2819.
[37] J. Wang, Y.Z. Xu, Y.F. Fu, X.D. Liu, Latent curing systems stabilized by reaction equilibrium in homogeneous mixtures of benzoxazine and amine, Sci. Rep. 6 (2016) 38584.
[38] B. Akkus, B. Kiskan, Y. Yagci, Counterion effect of amine salts on ring-opening polymerization of 1,3-benzoxazines, Macromol. Chem. Phys. 0(0) 1800268.
[39] G. Kaya, B. Kiskan, Y. Yagci, Phenolic naphthoxazines as curing promoters for benzoxazines, Macromolecules 51 (5) (2018) 1688–1695.
[40] W. Zhang, P. Froimowicz, C.R. Arza, S. Ohashi, Z. Xin, H. Ishida, Latent catalyst-containing naphthoxazine: synthesis and effects on ring-opening polymerization, Macromolecules 49 (19) (2016) 7129–7140.
[41] R. Andreu, J.A. Reina, J.C. Ronda, Carboxylic acid-containing benzoxazines as efficient catalysts in the thermal polymerization of benzoxazines, J. Polym. Sci. Part A-Polym. Chem 46 (18) (2008) 6091–6101.
[42] H. Ishida, Y. Rodriguez, Catalyzing the curing reaction of a new benzoxazine-based phenolic resin, J. Appl. Polym. Sci. 58 (10) (1995) 1751–1760.
[43] J. Dunkers, H. Ishida, Reaction of benzoxazine-based phenolic resins with strong and weak carboxylic acids and phenols as catalysts, J. Polym. Sci. Part A-Polym. Chem 37 (13) (1999) 1913–1921.
[44] P. Froimowicz, K. Zhang, H. Ishida, Intramolecular hydrogen bonding in benzoxazines: when structural design becomes functional, Chem. Eur. J. 22 (8) (2016) 2691–2707.
[45] K. Zhang, L. Han, P. Froimowicz, H. Ishida, A smart latent catalyst containing o-trifluoroacetamide functional benzoxazine: precursor for low temperature formation of very high performance polybenzoxazole with low dielectric constant and high thermal stability, Macromolecules 50 (17) (2017) 6552–6560.
[46] M. Baqar, T. Agag, R. Huang, J.o. Maia, S. Qutubuddin, H. Ishida, Mechanistic pathways for the polymerization of methylol-functional benzoxazine monomers, Macromolecules 45 (20) (2012) 8119–8125.
[47] M. Baqar, T. Agag, H. Ishida, S. Qutubuddin, Methylol-functional benzoxazines as precursors for high-performance thermoset polymers: unique simultaneous addition and condensation polymerization behavior, J. Polym. Sci. A Polym. Chem. 50 (11) (2012) 2275–2285.
[48] K. Zhang, L. Han, P. Froimowicz, H. Ishida, Synthesis, polymerization kinetics and thermal properties of para-methylol functional benzoxazine, React. Funct. Polym. 129 (2018) 23–28.
[49] S.N. Kolanadiyil, M. Minami, T. Endo, Synthesis and thermal properties of difunctional benzoxazines with attached oxazine ring at the para-, meta-, and ortho-position, Macromolecules 50 (9) (2017) 3476–3488.
[50] L. Zhang, Y.T. Zheng, R.T. Fu, Y.X. Chen, X.D. Liu, Contribution of blocking positions on the curing behaviors, networks and thermal properties of aromatic diamine-based benzoxazines, Thermochim. Acta 668 (2018) 65–72.
[51] P. Froimowicz, C. Rodriguez Arza, S. Ohashi, H. Ishida, Tailor-made and chemically designed synthesis of coumarin-containing benzoxazines and their reactivity study toward their thermosets, J. Polym. Sci. A Polym. Chem. 54 (10) (2016) 1428–1435.
[52] R. Lin, Y. Zhu, Y. Zhang, L. Wang, S. Yu, Pyrogallol-based benzoxazines with latent catalytic characteristics: the temperature-dependent effect of hydrogen bonds on ring-opening polymerization, Eur. Polym. J. 102 (2018) 141–150.
[53] C.L. Allen, A.R. Chhatwal, J.M. Williams, Direct amide formation from unactivated carboxylic acids and amines, Chem. Commun. 48 (5) (2012) 666–668.
[54] K.D. Demir, B. Kiskan, B. Aydogan, Y. Yagci, Thermally curable main-chain benzoxazine prepolymers via polycondensation route, React. Funct. Polym 73 (2) (2013) 346–359.
[55] T. Agag, J. Liu, R. Graf, H.W. Spiess, H. Ishida, Benzoxazole resin: a novel class of thermoset polymer via smart benzoxazine resin, Macromolecules 45 (22) (2012) 8991–8997.
[56] B. Kiskan, B. Koz, Y. Yagci, Synthesis and characterization of fluid 1,3-benzoxazine monomers and their thermally activated curing, J. Polym. Sci. A Polym. Chem. 47 (24) (2009) 6955–6961.
[57] M. Arslan, B. Kiskan, Y. Yagci, Benzoxazine-based thermosets with autonomous self-healing ability, Macromolecules 48 (5) (2015) 1329–1334.
[58] W.K. Zhang, X.X. Gao, L.L. Yu, Y.R. Ren, H. Xu, B.Y. Liu, Y.P. Wang, X.M. Fang, Y.Q. Xu, T. Ding, Silane-functional benzoxazine: synthesis, polymerization kinetics and thermal stability, Polym. Int. 66 (6) (2017) 908–915.
[59] K. Zhang, H. Ishida, An anomalous trade-off effect on the properties of smart ortho-functional benzoxazines, Polym. Chem. 6 (13) (2015) 2541–2550.
[60] T. Agag, C.R. Arza, F.H. Maurer, H. Ishida, Crosslinked polyamide based on main-chain type polybenzoxazines derived from a primary amine-functionalized benzoxazine monomer, J. Polym. Sci. A Polym. Chem. 49 (20) (2011) 4335–4342.
[61] H.E. Kissinger, Reaction kinetics in differential thermal analysis, Anal. Chem. 29 (11) (1957) 1702–1706.
[62] T. Ozawa, Kinetics of non-isothermal crystallization, Polymer 12 (3) (1971) 150–158.
[63] Y. Liu, C. Liao, Z. Hao, X. Luo, S. Jing, M. Run, The polymerization behavior and thermal properties of benzoxazine based on o-allylphenol and 4,4′-diaminodiphenyl methane, React. Funct. Polym. 75 (2014) 9–15.